Processes leading to extreme seasons

– research at the weather-climate interface based on reanalyses and large ensemble climate simulations

Heini Wernli, Urs Beyerle, Hanin Binder, Maxi Boettcher, Erich Fischer, Emmanouil Flaounas, Christoph Frei, Katharina Hartmuth, Mauro Hermann, Hanna Joos, Reto Knutti, Flavio Lehner, Lukas Papritz, Matthias Röthlisberger, Michael Sprenger, and Philipp Zschenderlein

see also www.intexseas.ch

EGU, 26 May 2022

Motivation

nature geoscience

LETTERS

PUBLISHED ONLINE: 19 OCTOBER 2015 | DOI: 10.1038/NGEO2561

Weather chains during the 2013/2014 winter and their significance for seasonal prediction

Huw C. Davies

ELSEVIER

Climate Risk Management

journal homepage: www.elsevier.com/locate/crm

Past and future climate change in the context of memorable seasonal extremes

T. Matthews [a,*], D. Mullan [b], R.L. Wilby [c], C. Broderick [d], C. Murphy [d]

Winter 2010 in Europe: A cold extreme in a warming climate

J. Cattiaux,[1] R. Vautard,[1] C. Cassou,[2] P. Yiou,[1] V. Masson-Delmotte,[1] and F. Codron[3]

Multiple Causes of the North American Abnormal Winter 1976–77[1]

Jerome Namias

Many case studies about "extreme seasons", their socio-economic impact and underlying dynamics, BUT …

- can extreme seasons be identified objectively?
- do extreme seasons share common characteristics and processes?

Overview

Extreme season identification: rationale and methodology

Data: ERA5 and CESM-LENS (with 6-h 3-d output to study weather systems)

Example applications

- Extreme seasons in ERA5
- CESM-LENS analogues of observed extreme seasons
- Substructure of extreme seasons
- Arctic extreme seasons: boundary forcing vs. internal variability
- Climate change effects on wettest seasons

Weather system dynamics in CESM-LENS: cyclones, warm conveyor belts, blocks, Rossby wave breaking, Alpine foehn

Overview

Extreme season identification: rationale and methodology

Data: ERA5 and CESM-LENS (wi[illegible]put to study weather systems)

Example applicatio[illegible]

- Extreme sea[illegible]RA5
- CESM-LENS analogues of observed extreme seasons
- Substructure of extreme seasons
- Arctic extreme seasons: boundary forcing vs. internal variability
- Climate change effects on wettest seasons

See supplementary material

Weather system dynamics in CESM-LENS: cyclones, warm conveyor belts, blocks, Rossby wave breaking, Alpine foehn

Extreme season identification scheme

Step 1: Grid point-wise statistical modelling of seasonal mean distributions to calculate the local return period (LRP) for each seasonal mean value.

Use Yeo-Johnson transformed normal distribution (N^{YJ}), which allows modelling skewed seasonal mean T2m distributions.

Step 2: Identify locally extreme seasonal mean values with criterion LRP > $\tau = 40$ years.

Step 3: Form spatially coherent extreme season objects with LRP > τ, and quantify their characteristics such as size and intensity.

→ Röthlisberger et al. 2021 (J. Clim.)

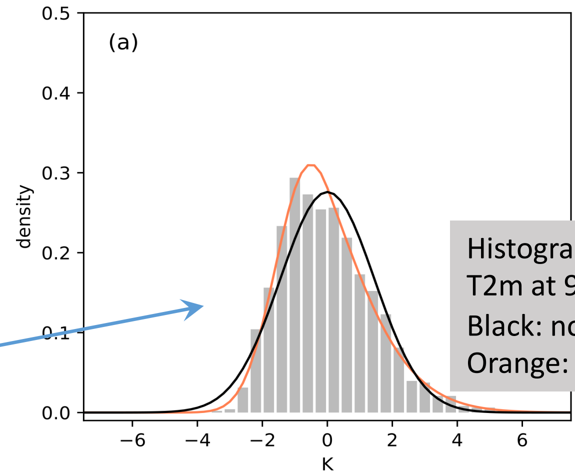

Histogram of CESM-LENS JJA T2m at 98°W/37°N.
Black: normal distribution fit
Orange: N^{YJ} fit

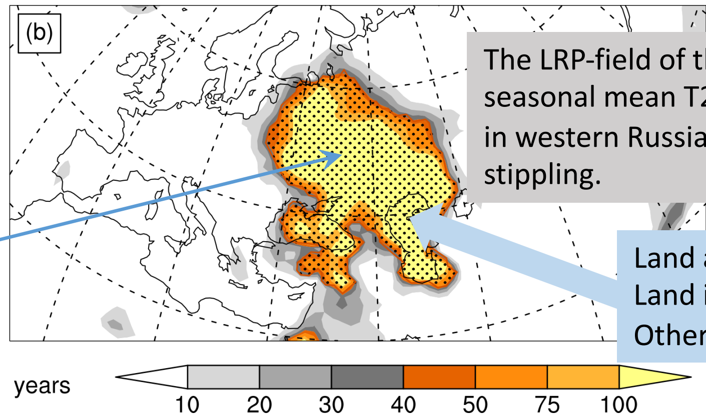

The LRP-field of the 2010 JJA seasonal mean T2m. The T_{JJA+} object in western Russia is highlighted with stippling.

Land area: 3.85 x 10^6 km^2
Land intensity: 2.92 K
Other characteristics: …

Example application in ERA5

Identify 10 largest cold winters (land area only)

Events include:

DJF 2009/2010 in W Siberia
(e.g., Cohen et al. 2010, GRL)

DJF 2013/14 in eastern U.S.
(e.g., Davies 2015, Nature Geo)

→ Boettcher et al., in prep.

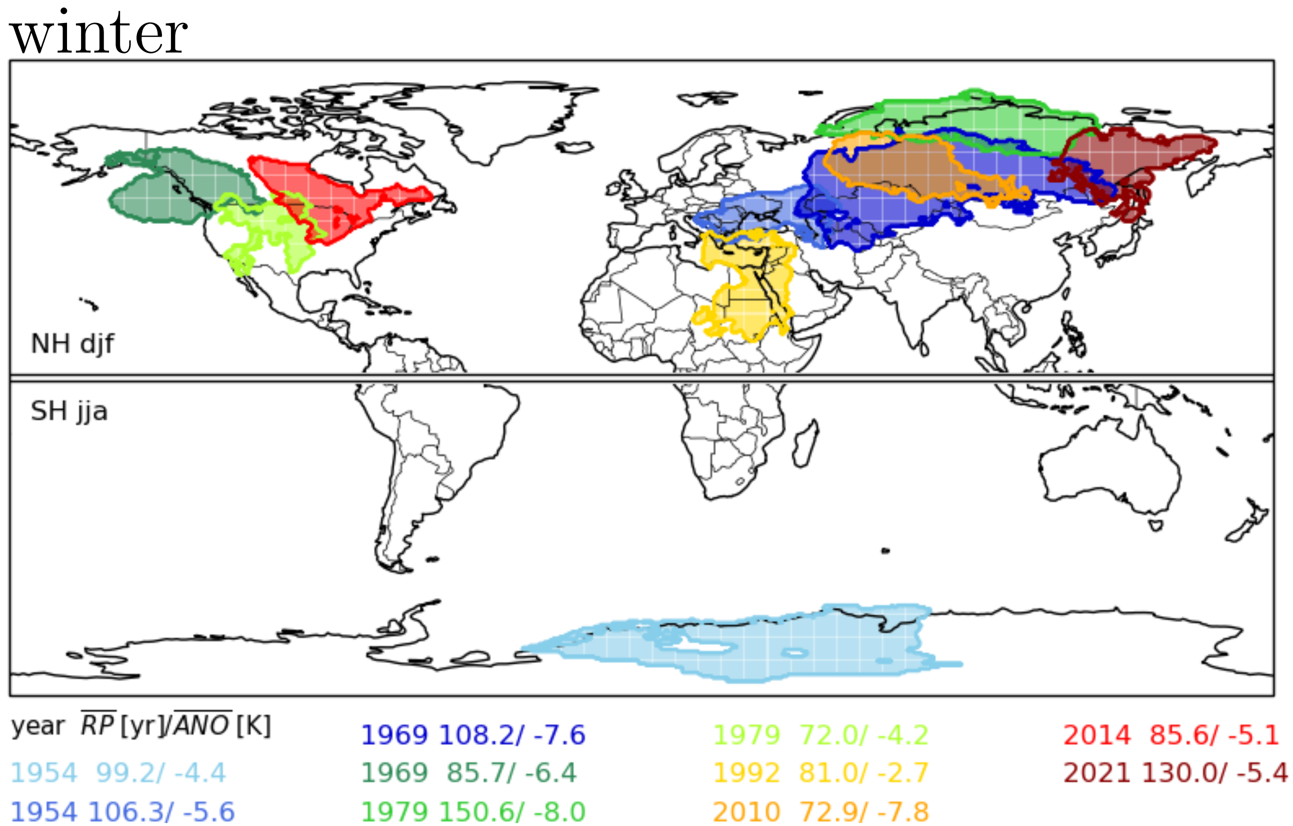

Example application in CESM-LENS (1/2)

Large set of CESM-LENS extreme seasons allows systematically analysing extreme seasons with comparable characteristics to observed events.

CESM-LENS "analogues" to cold winter 2013/14 in North America, i.e., simulated extreme season objects with comparable size and intensity characteristics.

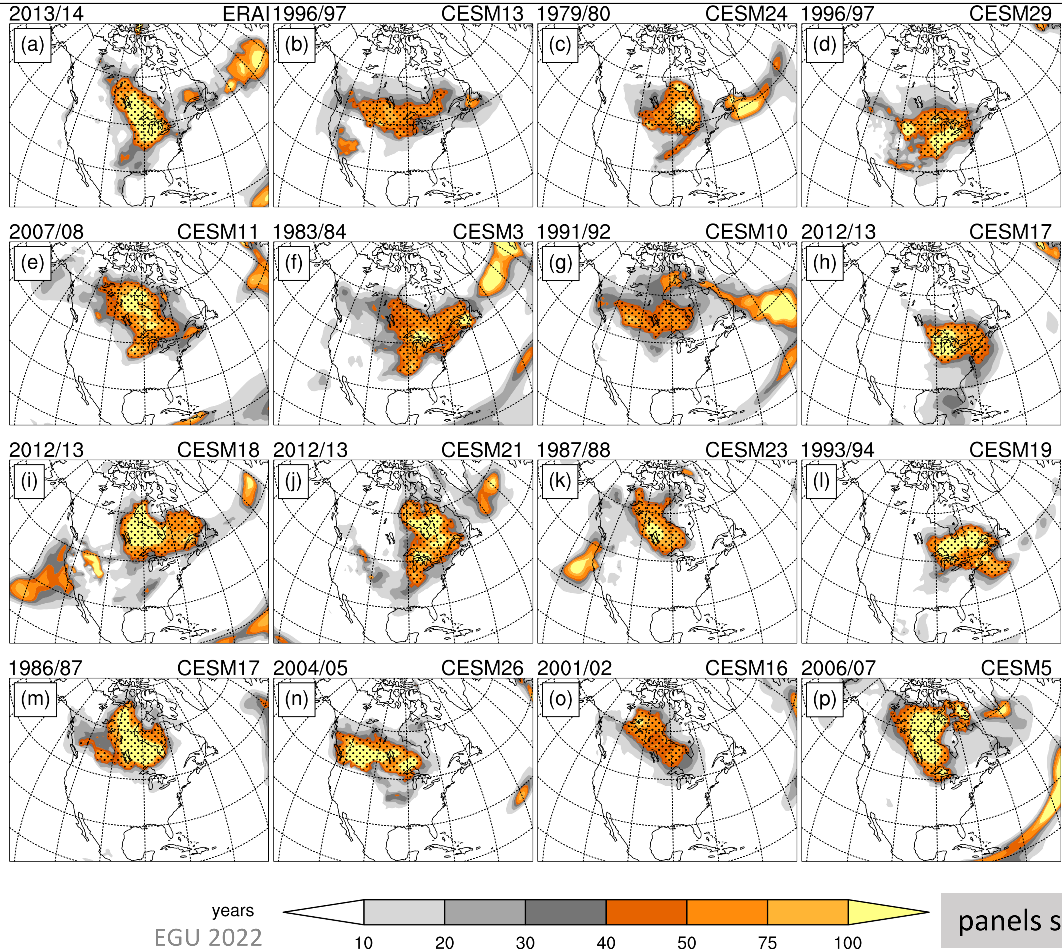

panels show LRP (years)

Example application in CESM-LENS (2/2)

Hartmann (2015): cold winter 2013/14 in N. America was in part forced by anomalous SST pattern

Composite SST anomalies from the 15 analogues indeed shows characteristics similar to the obs. in 2013/14 – but, some analogues have a completely different SST anomaly pattern

CESM-LENS analogues suggest that the observed 2013/14 SST anomaly pattern is a frequent characteristic – but not a necessary condition - of extremely cold N. American winters → Röthlisberger et al. 2021, J. Clim.

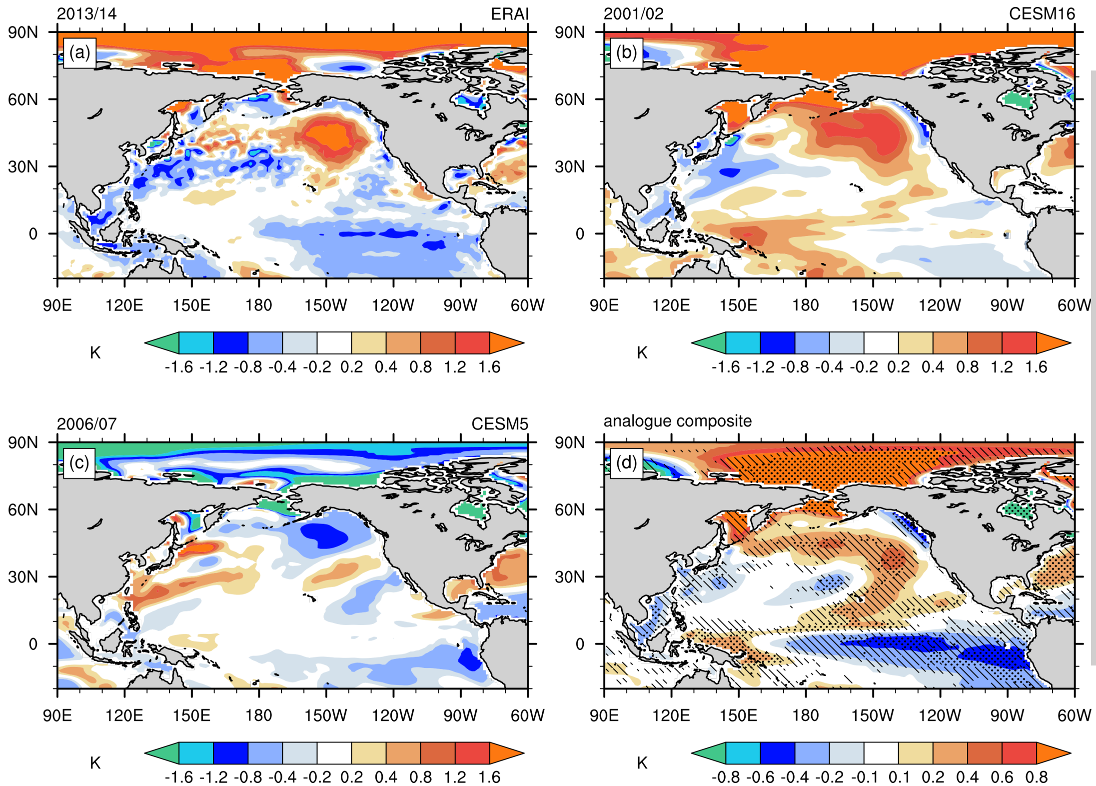

(a) SST anomalies during DJF 2013/14. (b,c) SST anomalies for two selected CESM-LENS analogues and (d) composite SST anomalies for all 15 analogues. Hatching and stippling indicates grid points where the SST anomalies in at least 10 and 12 analogues have the same sign, respectively.

Find more in the supplementary material and in our publications …

Flaounas, E., M. Röthlisberger, M. Boettcher, M. Sprenger, and H. Wernli, 2021. Extreme wet seasons – their definition and relationship with synoptic-scale weather systems. Weather Clim. Dynam., 2, 71–88.

Hartmuth, K., M. Boettcher, H. Wernli, and L. Papritz, 2022. Identification, characteristics and dynamics of Arctic extreme seasons. Weather Clim. Dynam., 3, 89–111.

Röthlisberger, M., M. Sprenger, **E. Flaounas**, U. Beyerle, and H. Wernli, 2020. The substructure of extremely hot summers in the Northern Hemisphere. Weather Clim. Dynam., 1, 45–62.

Röthlisberger, M., M. Hermann, C. Frei, F. Lehner, E. M. Fischer, R. Knutti, and H. Wernli, 2021. A new framework for identifying and investigating seasonal climate extremes. J. Climate, 34, 7761–7782.

Zschenderlein, P., and H. Wernli, 2022. How intense daily precipitation depends on temperature and the occurrence of specific weather systems – an investigation with ERA5 reanalyses in the extratropical Northern Hemisphere. Weather Clim. Dynam., 3, 391–411.

More at: www.intexseas.ch

→ new EGU/Copernicus open access journal

Supplementary material

Slides 11-14: Rationale and identification method (longer version)
Röthlisberger et al. 2021, J. Clim.

Slides 15-22: Extreme season substructure
Röthlisberger et al. 2020, WCD

Slides 23-27: Climate change effects on wettest seasons

Slides 28-31: Arctic extreme seasons
Hartmuth et al. 2022, WCD

Slides 32-41: Weather systems and climate change

Rationale and identification method

Röthlisberger et al. 2021 (J. Clim.)

Extreme seasons identification: Rationale

Seasonal climate extremes, such as extremely hot summers or cold winters, have large socio-economic impacts, but due to their rareness they are difficult to study beyond individual case studies. Consequently, climatological characteristics, i.e., characteristics that are shared by a large number of seasonal extremes, are poorly studied and poorly understood.

- In this concept study we develop a spatial pooling strategy for seasonal extreme events that allows analysing larger samples of comparable seasonal extreme events, using the example of extremely hot summers and cold winters (hereafter T_{JJA+} and T_{DJF-} events, respectively).
- The centrepiece of our approach is an extreme season identification scheme that identifies spatial extreme season objects in reanalysis and climate model data based on grid point wise statistical modelling of seasonal two meter temperature (T2m) means.
- Applying the scheme to 40 years of data from ERA-Interim and 1200 years from CESM-LENS yields large sets of T_{JJA+} and T_{DJF-} events that allow studying such seasonal climate extremes in hitherto unexplored ways.

Extreme season identification scheme

DETAILED VERSION (1/2)

- **Statistical modelling of seasonal means:** Previous studies used a normal distribution to model seasonal mean temperatures (e.g., Chase, 2006; Barriopedro et al. 2011). However, at the grid point scale, seasonal mean T2m distributions are often skewed. Therefore, we incorporate the Yeo-Johnson transform (Yeo and Johnson, 2000) into the normal distribution and model JJA and DJF T2m data with a Yeo-Johnson transformed normal distribution (hereafter N^{YJ}) with cdf

- $G(x; \mu, \sigma^2, \lambda) = F(k(x;\ \lambda);\ \mu, \sigma^2)$

- where $k(x;\ \lambda)$ is the Yeo-Johnson power transform of the variable x with transformation parameter λ, and $F(y;\ \mu, \sigma^2)$ is the cdf of the normal distribution.

- This statistical model allows describing positively and negatively skewed seasonal mean T2m distributions and allows to model seasonal mean T2m over a wide range of climates (an example for a grid point in North America is shown on the right).

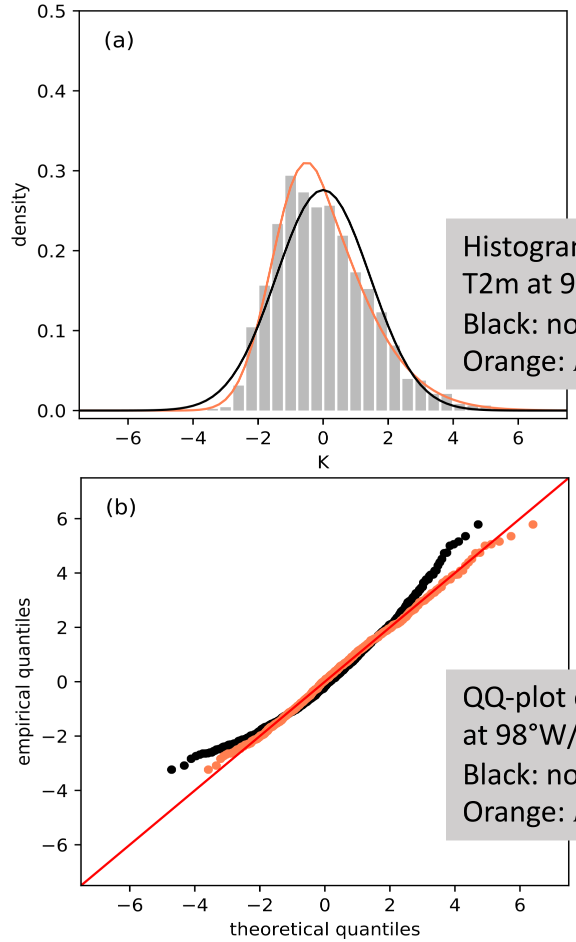

Histogram of CESM-LENS JJA T2m at 98°W/37°N.
Black: normal distribution fit
Orange: N^{YJ} fit

QQ-plot of CESM-LENS JJA T2m at 98°W/37°N.
Black: normal distribution fit
Orange: N^{YJ} fit

Extreme season identification scheme

DETAILED VERSION (2/2)

- **Forming extreme season objects:** From the N^{YJ}-fit at each grid point we compute local return periods (LRPs) for each seasonal mean value. Seasonal mean values are deemed "extreme" if their LRP exceeds 40 years. Extreme season objects are then constructed as connected regions where the LRP exceeds 40 years. For each extreme season object we compute a number of characteristics (area, centre of mass, an intensity measure etc.). The formation of extreme season objects is illustrated below for the T_{JJA+} object of the hot western Russian summer in 2010.

Panels (a,b) show the LRP-field of the 2010 JJA seasonal mean T2m, which is derived from the grid point wise N^{YJ}-fit. In (b) the T_{JJA+} object in western Russia is highlighted with stippling. The land area and an intensity measure, computed as the area weighted mean T2m anomaly over all land grid points of the object, are given below.

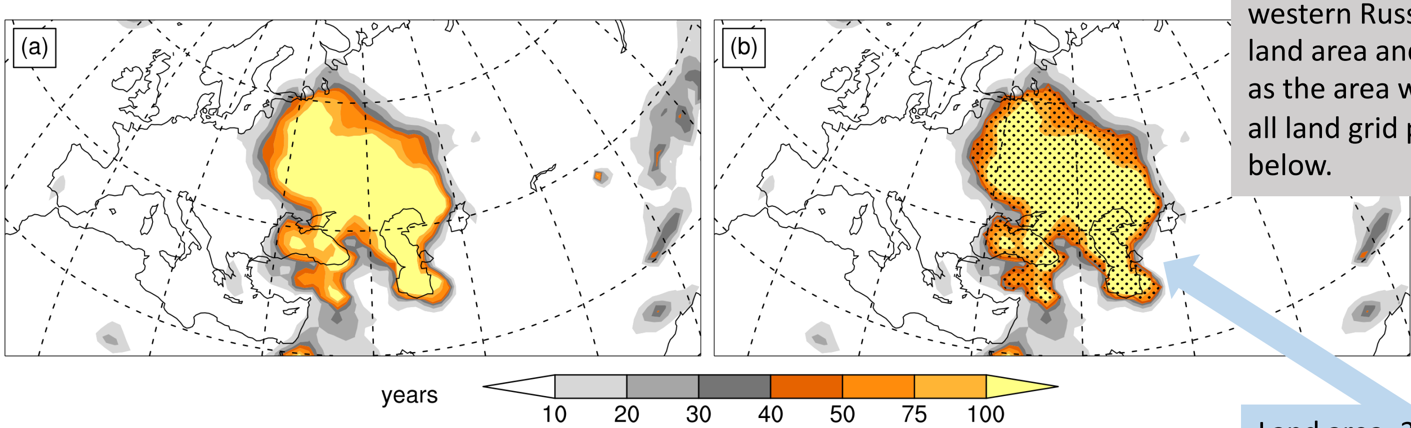

Land area: 3.85 x 10^6 km^2
Land intensity: 2.92 K
Other characteristics: …

Extreme summer substructure

Röthlisberger et al. 2020 (WCD)

The substructure of an (extreme) summer

Hot temperature extremes on close to seasonal time scales can have severe ecological, public health and economic effects that sometimes go beyond (or are distinct from) the effects of temperature extremes on synoptic (e.g., multi-day) time scales.

An extremely hot summer (hereafter extreme summer) may be defined in the upper tail of the June–August (JJA) seasonal mean T2m distribution. However, when doing so it is unclear whether a particular summer is extreme because of an unusual heat wave (i.e., hottest summer days hotter than climatologically), a suppression of cool summer days, a shift in the entire temperature distribution or any combination of the above.

However, these different extreme summer substructures conceivably shape the societal impact of an extreme summer. In this study we therefore assess which part of the local T2m distribution contributes how much to extreme summers defined in the upper tail of the JJA seasonal mean T2m distribution.

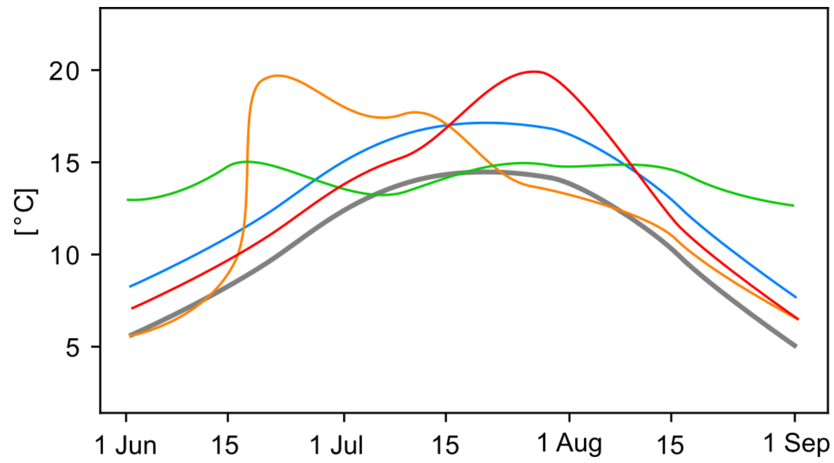

Archetypical substructures:
Heat wave during an otherwise benign summer
Milder than normal cool summer days
Shift in the entire T2m distribution
Any combination of the above
Gray line = climatological temperature evolution

The substructure of an (extreme) summer

example from ERA-I grid point at 9°E/47°N

Research question: Which part of the local T2m distribution contributes how much to the temperature anomalies during extremely hot summers?

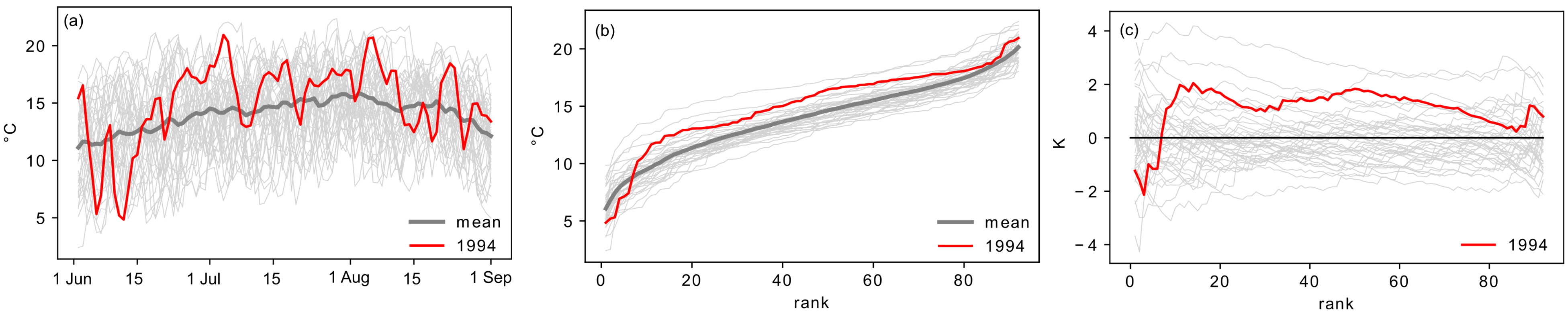

Step 1: Rank all T2m values within their respective season

Step 2: Compute "rank day means"

Step 3: Compute "rank day anomalies"

Integrating the rank day anomalies over all ranks exactly recovers the seasonal anomaly

Method to assess the substructure of an (extreme) summer

example from ERA-I grid point at 9°E/47°N

Time evolution of T2m at 9°E/47°N for all summers in 1979–2018

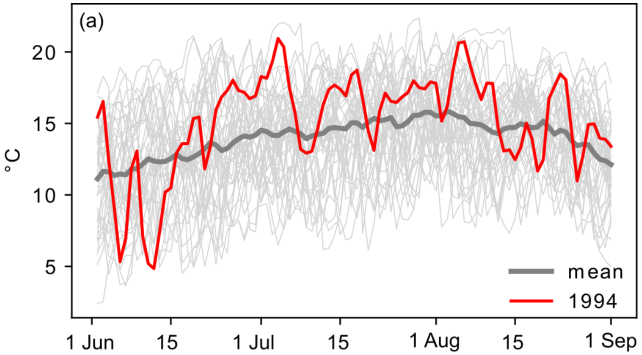

Daily mean T2m values ranked within their respective summer

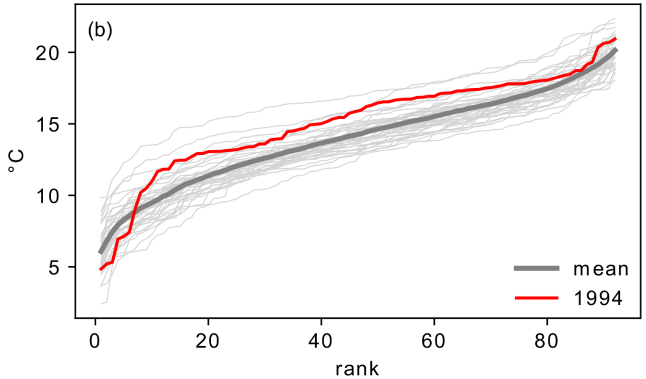

"Rank day anomaly" of each rank day in each season

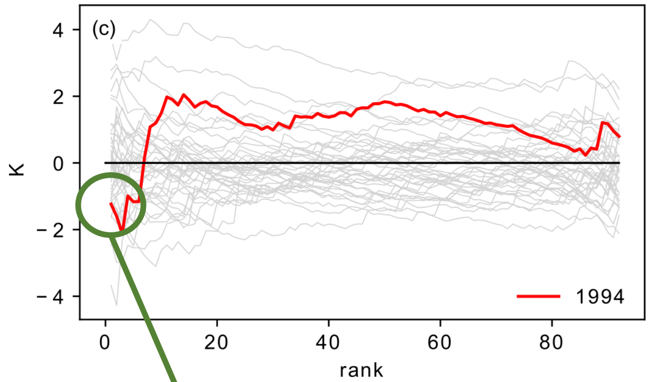

Step 1: Rank all T2m values within their respective season

Step 2: Compute "rank day means"

Step 3: Compute "rank day anomalies"

The coldest day of the 1994 summer was 1.2 K colder than the average coldest summer day at this grid point.

Integrating the rank day anomalies over the coldest, middle and hottest tercile of summer days exactly quantifies the contributions from these three thirds of the summer days to the seasonal mean anomaly.

Applying this decomposition to extreme summers allows for quantifying their substructures.

Two example grid points
ERA-Interim

(left) Hot days make summers extreme

(right) Cold days particularly important

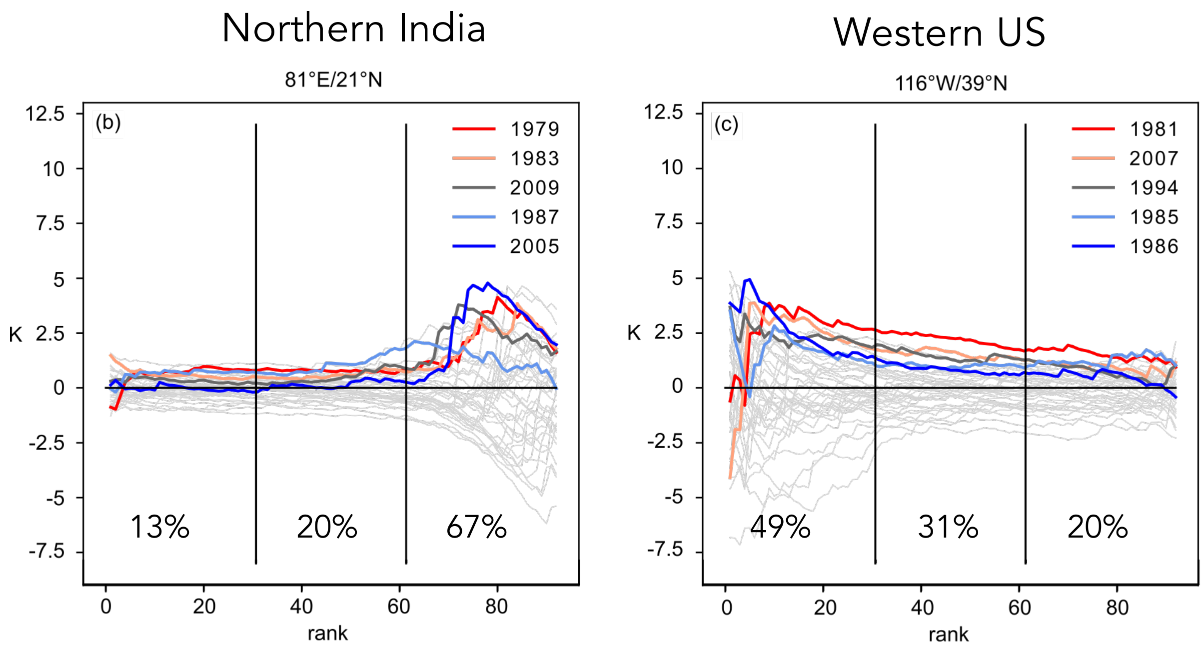

Two example grid points
CESM-LENS

Gray: 5th to 95th percentile of all JJA seasons
Red dotted: max, min of exseas
Red dashed: q10, q90 of exseas
Red solid: median of exseas

Excellent agreement between ERAI & CESM substructures at these grid points!

How about other regions?

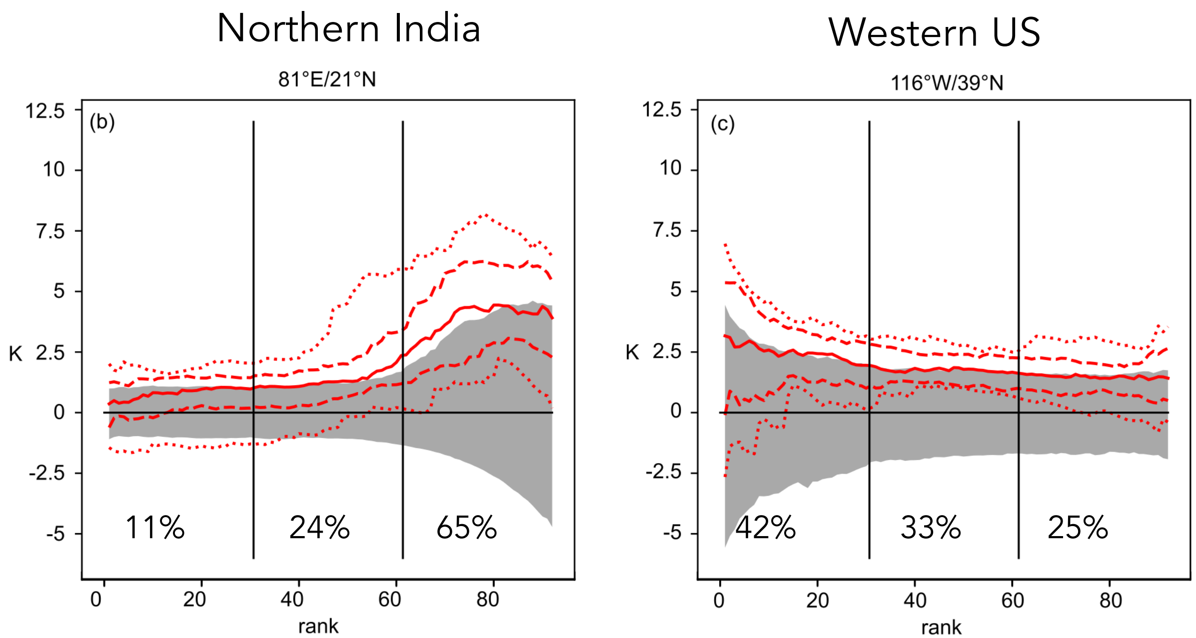

Spatial variability
ERAI vs. CESM-LENS

Contributions to extreme summer temperature anomalies from the 30 coldest and 30 hottest days of each summer.

Key findings:

- Large spatial variability in these contributions
- In some regions, the suppression of cold summer days is more important for extreme summers than the occurrence of heat waves
- Remarkable qualitative (and partly even quantitative) agreement between ERAI and CESM-LENS

hot days
ERAI

hot days
CESM

cold days
ERAI

cold days
CESM

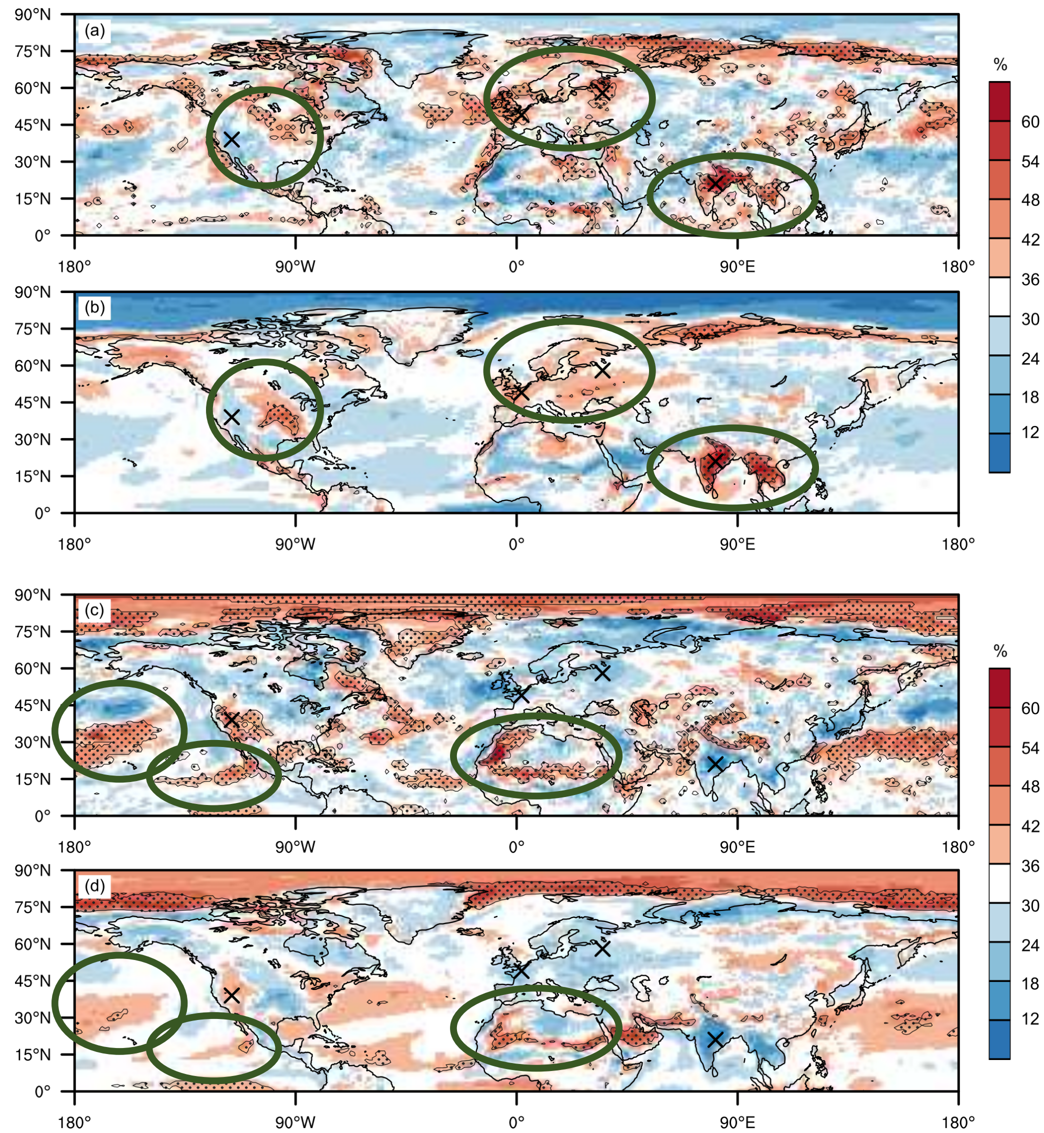

Summary and conclusions

- The substructure of extreme summers is assessed by decomposing the seasonal mean anomaly into the contributions from all rank days.
- Large spatial variability in extreme summer substructures.
- Suppression of cool summer days is fundamentally important for seasonal (JJA) temperature extremes.
- CESM reliably reproduces the ERA-I extreme summer substructures and may therefore be used to assess changes in extreme summer substructures with climate change.
- Physical processes that shape the local extreme summer substructure differ widely in space, and may be related to e.g., monsoons, physical boundaries such as sea ice edges, orography and Rossby wave dynamics or the location of climatological temperature gradients [more on that in the paper].

Acknowledgements: This work was funded by the European Research Council under the European Union's Horizon 2020 research and innovation programme (INTEXseas project, grant nr. 787652). Moreover, Maxi Böttcher and Lukas Papritz (both ETH Zürich) are acknowledged for helpful discussions during different stages of this work and Gary Strand and Clara Deser (both NCAR) for providing CESM restart files.

Climate change effects on wettest seasons

Zschenderlein and Wernli, in prep.

Climate change effects on wettest seasons

Simple identification of wettest seasons in CESM-LENS: 10 wettest DJF seasons at every grid point

Decompose wet season anomaly P^* (i.e., deviation from climatological mean) into contributions from increased

- wet day frequency N_{wet} → more wet days in wettest seasons?
- wet day intensity P_{int} → more intense daily precipitation in wettest seasons?
- non-linear term

$$P^* = N^*_{wet}\ \overline{P_{int}} + \overline{N_{wet}}\ P^*_{int} + N^*_{wet}\ P^*_{int}$$

Investigate

- which term dominates where and when?
- does relative importance of terms change in future climate?

Decomposition of anomalies in wettest season

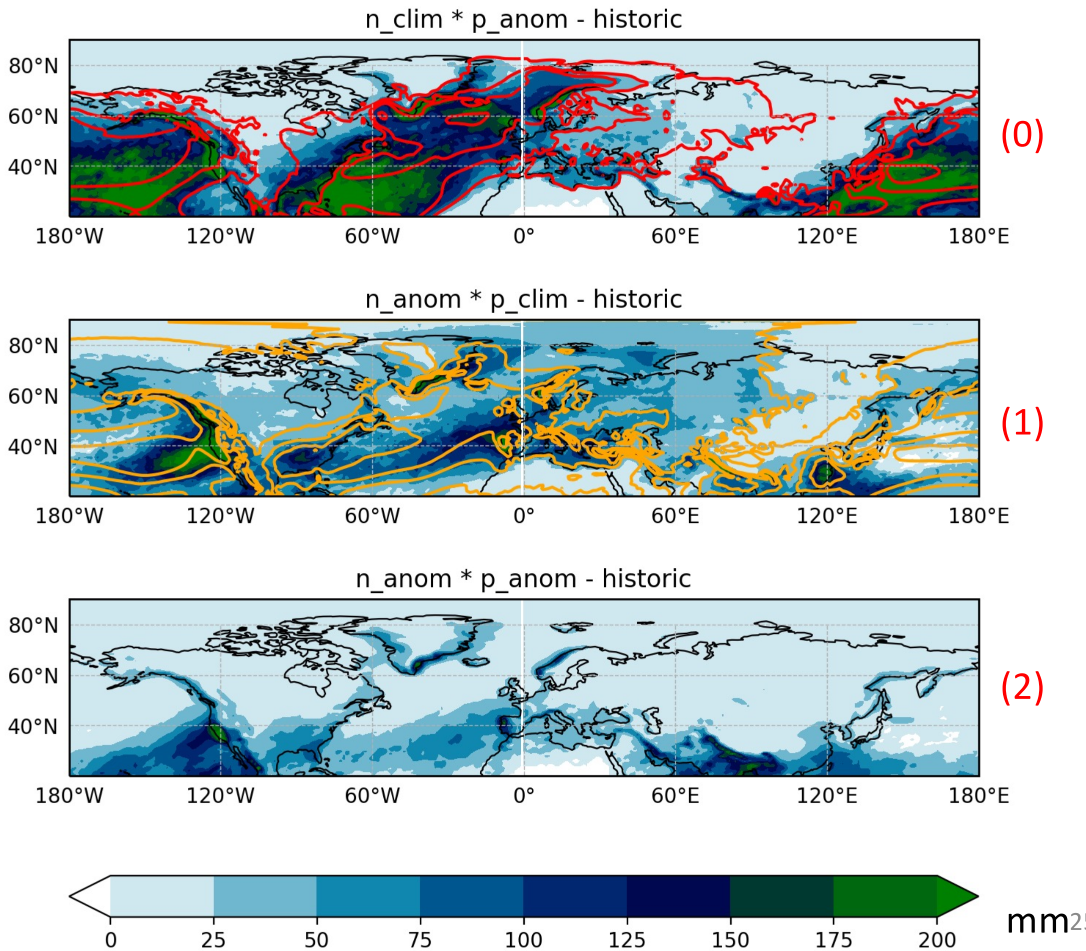

Red contours: $\overline{N_{wet}}$ [20,40,60,80 d]

Orange contours: $\overline{P_{nt}}$ [2,4,6,8 mm d^{-1}]

$$P^* = N^*_{wet}\,\overline{P_{int}} + \overline{N_{wet}}\,P^*_{int} + N^*_{wet}\,P^*_{int}$$

(1) (0) (2)

Which term dominates?

CESM-LENS historic climate (1991-2000), DJF

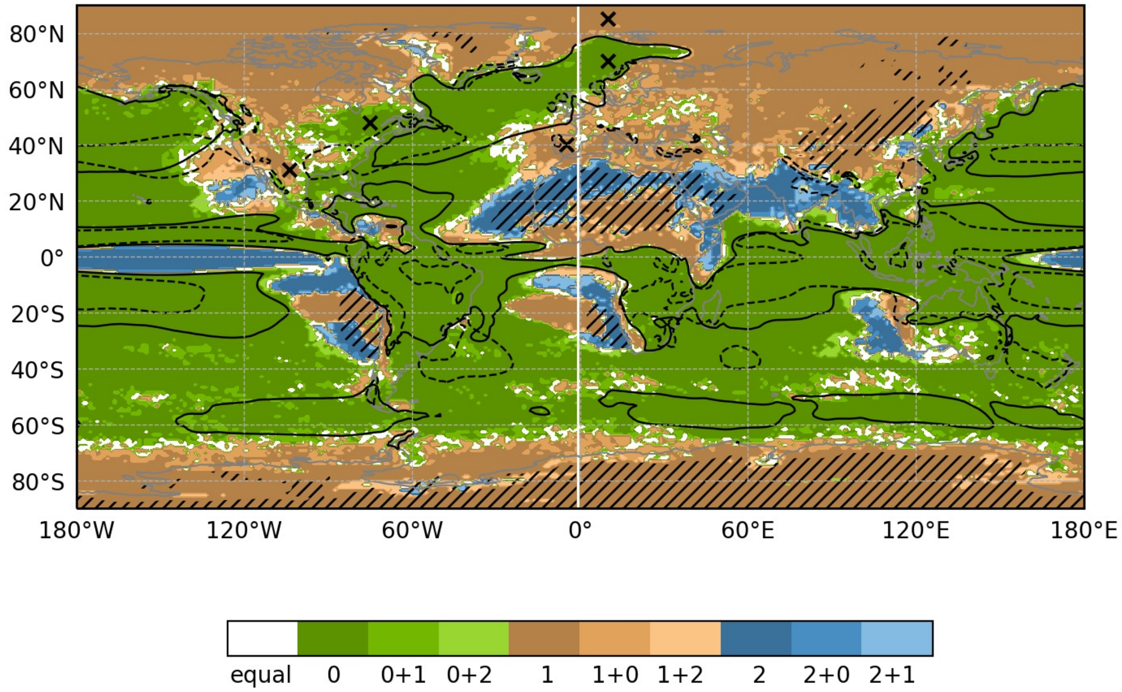

$$P^* = \underbrace{\boxed{N^*_{wet}\ \overline{P_{int}}}}_{(1)} + \underbrace{\boxed{\overline{N_{wet}}\ P^*_{int}}}_{(0)} + \underbrace{\boxed{N^*_{wet}\ P^*_{int}}}_{(2)}$$

→ different processes lead to wettest seasons in different regions

Which term dominates?

CESM-LENS future climate (2091-2100), DJF

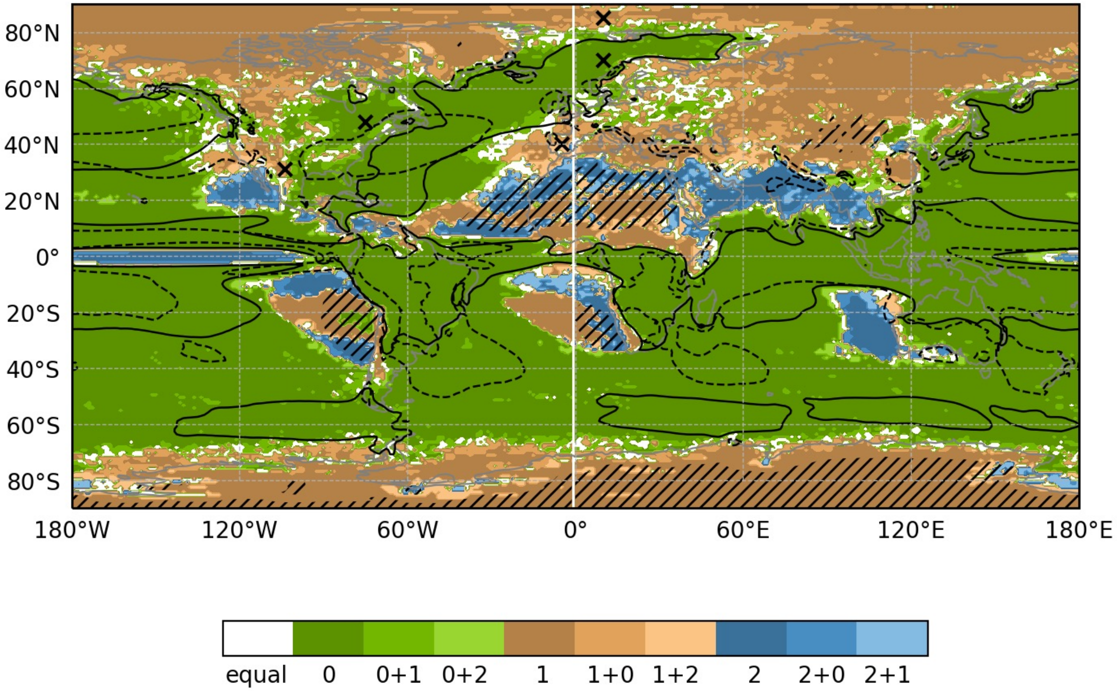

$$P^* = \boxed{N^*_{wet}\,\overline{P_{int}}} + \boxed{\overline{N_{wet}}\,P^*_{int}} + \boxed{N^*_{wet}\,P^*_{int}}$$

(1) (0) (2)

→ patterns are fairly robust with respect to global warming

Arctic extreme seasons

Hartmuth et al. 2022 (WCD)

Arctic extreme seasons

Identify extreme seasons with principal component analysis in 6-dimensional phase space of seasonal mean values of 2-m temperature, surface precipitation, and the 4 components of the surface energy balance: extreme seasons = outliers in the PC1/PC2 plane (see next slide)

The figures on the next slide show biplots in the PC1/PC2 plane with projections of the 6 basic variables (vectors) and dots for the seasonal mean values in (left) ERA5 and (right) CESM-LENS historic (1991-2000)

→ do this approach separately for different Arctic subregions (ice, ocean, mixed)

→ study substructure, weather systems and preconditioning of extreme seasons

Arctic extreme seasons

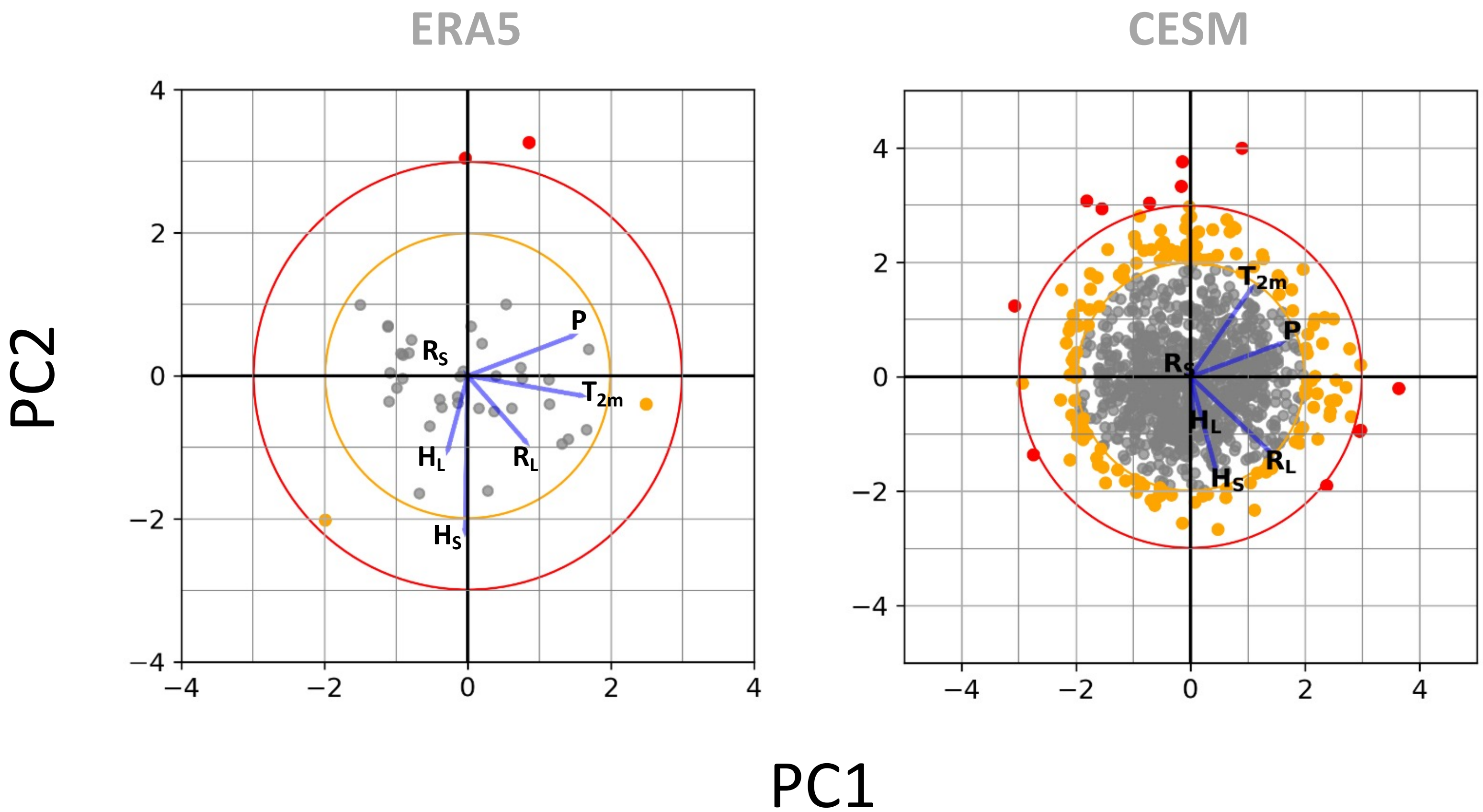

Arctic extreme seasons

Detailed case studies of extreme seasons in ERA5 (red dots in left diagram on previous slide)

→ extreme seasonal conditions in the Arctic are spatially heterogeneous, related to different near-surface parameters and caused by different synoptic-scale weather systems (cyclones, blocks, cold air outbreaks), potentially in combination with surface preconditioning due to anomalous ocean and sea ice conditions at the beginning of the season.

Weather system and climate change

We identified in CESM-LENS:

Warm conveyor belt (WCB) properties (Joos et al., in prep.)
→ WCBs become more intense and ascend to higher altitudes in future climate

WCBs and cyclone intensification (Binder et al., in prep.)
→ most intense cyclones become more diabatic (stronger WCB)

Foehn in Switzerland (Mony et al. 2021, Wea. Forecasting)
→ seasonally varying climate change effects

Warm Conveyor Belts in CESM-LENS

1) Changes in frequency of occurence from present day (1990-2000) to future (2091-2100) climate in DJF

WCB starting regions

WCB outflow regions

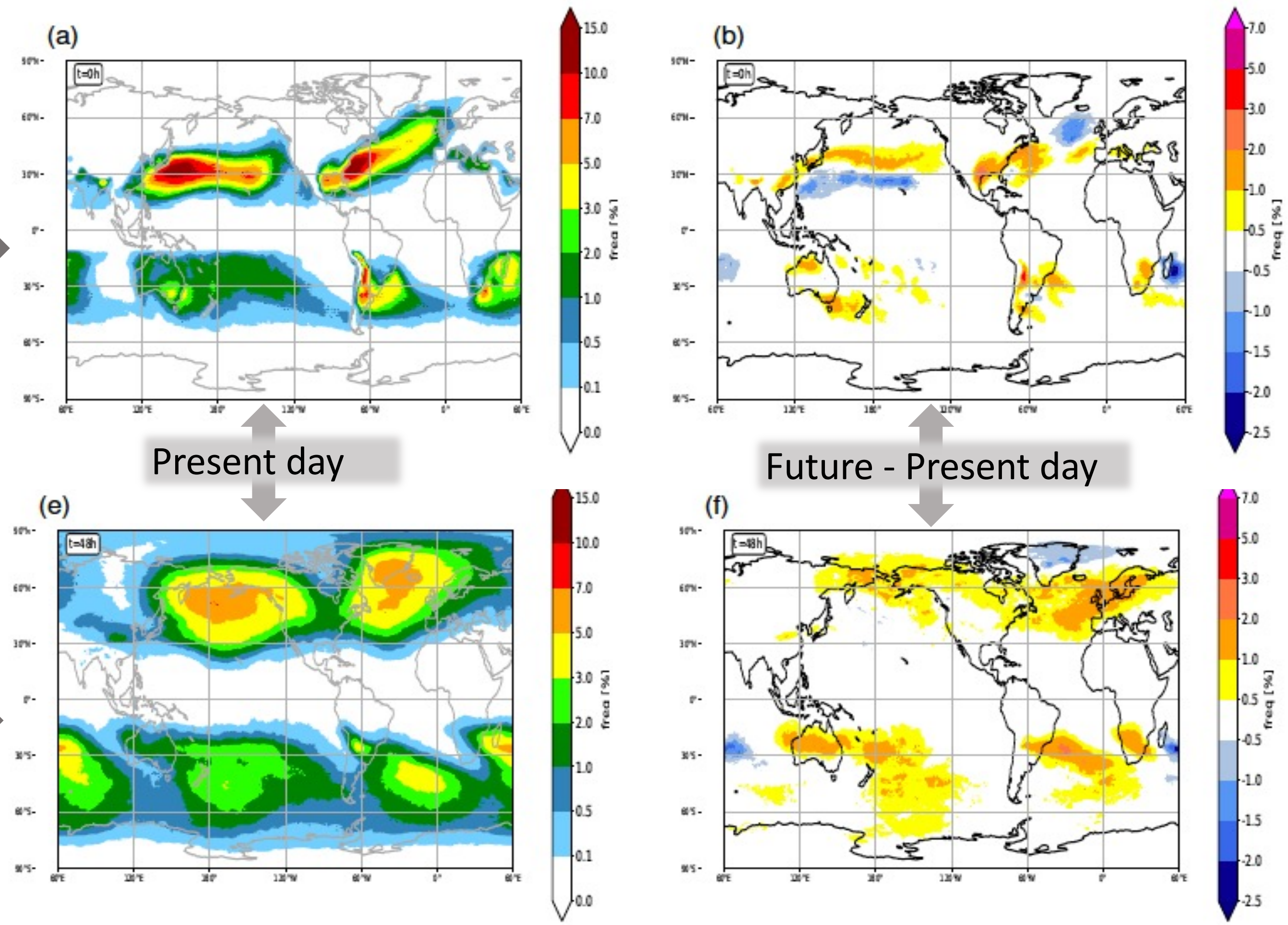

- Only small changes in frequency of occurence
- Different changes in North Pacific and North Atlantic

Warm Conveyor Belts in CESM-LENS

2) Changes in WCB characteristics from present day to future climate in DJF

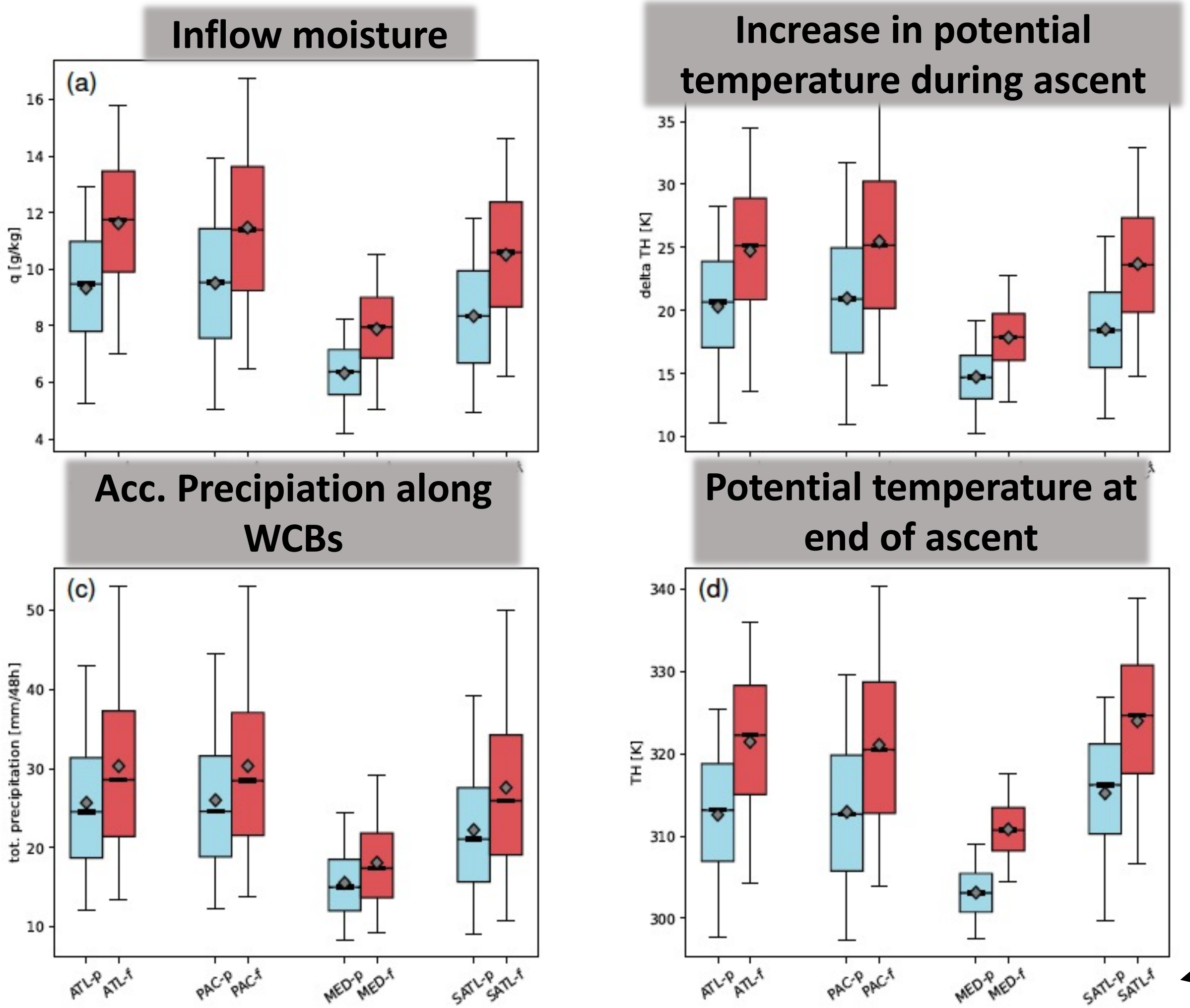

Present day

Future

WCBs in future are characterized by

- higher moisture content in inflow (a)
- increase in diabatic heating along ascending WCB (b)
- increase in associated precipitation (c)
- ascent to higher isentropes (d)

Analysis done for different regions: North Atlantic (ATL), North Pacific (PAC), Mediterranean (MED), South Atlantic (SATL)

Warm Conveyor Belts in CESM-LENS

3) Location of WCB outflow in present day and future climate in DJF in the North Atlantic

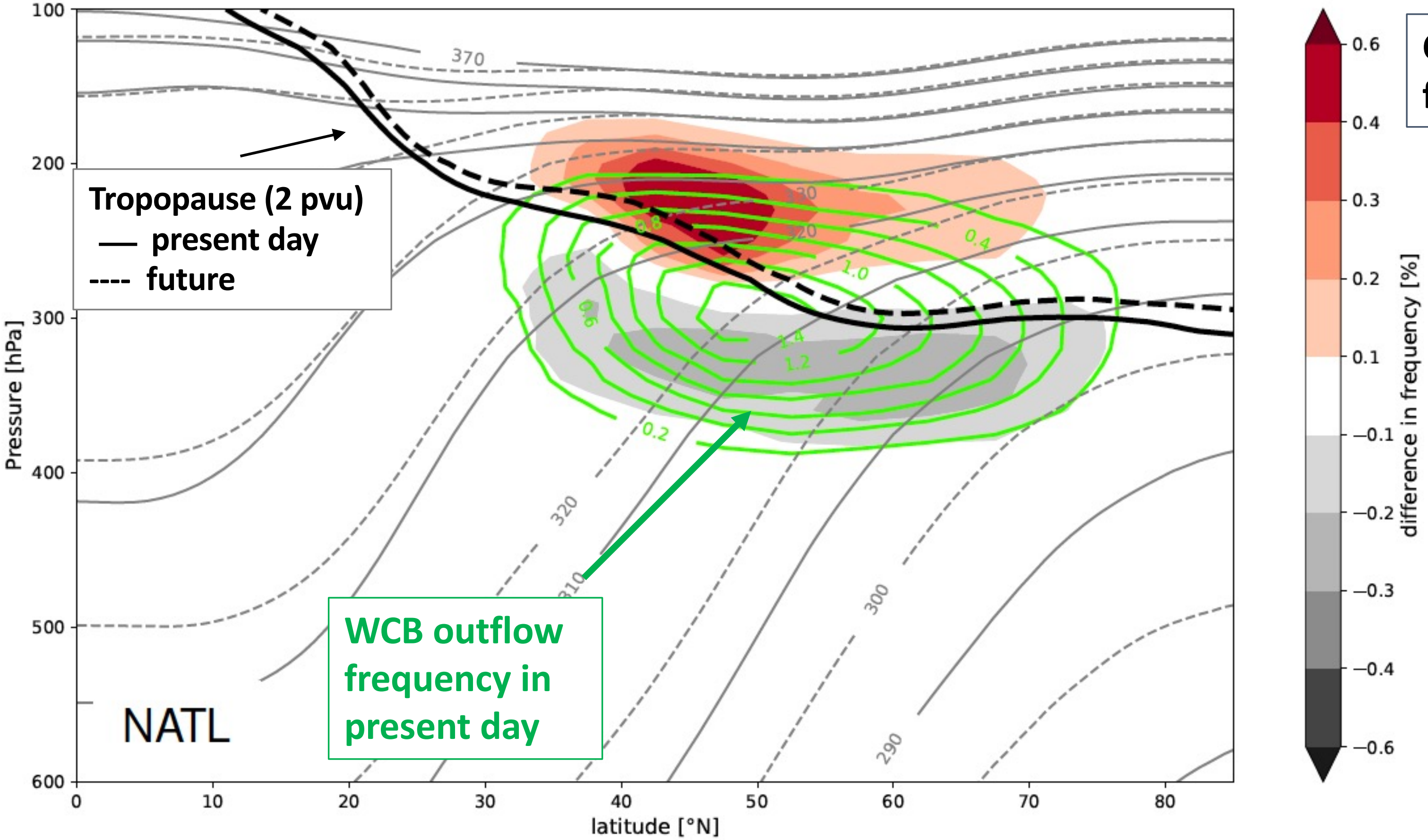

Colour: difference in outflow frequency future - present day

- Outflow in future shifted to higher altitudes (also seen in other regions)
- Only slight upward shift in position of tropopause in future

--> Impact on disturbance of wave guide ?

WCBs and their role for cyclone intensification in present-day and future climate simulations of CESM-LENS

Hanin Binder, Hanna Joos, Michael Sprenger and Heini Wernli

Motivation: WCBs are the main cloud and precipitation producing airstreams in extratropical cyclones (e.g., Browning 1990, Wernli and Davies 1997). The intense latent heating produces positive low-level potential vortictiy (PV) anomalies that often contribute to the intensification of the associated cyclone (Binder et al. 2016).

Research question: How does climate change affect the cyclones' WCB strength and the importance of WCB-related diabatic PV production for cyclone intensification?

Method: Identification of a large number of cyclones and their associated WCB trajectories in 50 years of present-day climate (CESM-HIST) and 50 years of future climate (CESM-RCP85) in both hemispheres during the winter season.

Measure for cyclone intensification: Latitude-adjusted max. value of ΔSLP of all 24h intervals along track, in Bergeron units (Sanders and Gyakum 1980)

Measure for WCB strength: WCB air mass with pressure > 500 hPa during the 24h of strongest cyclone intensification

How will WCB strength and cyclone deepening rate change in a future climate?

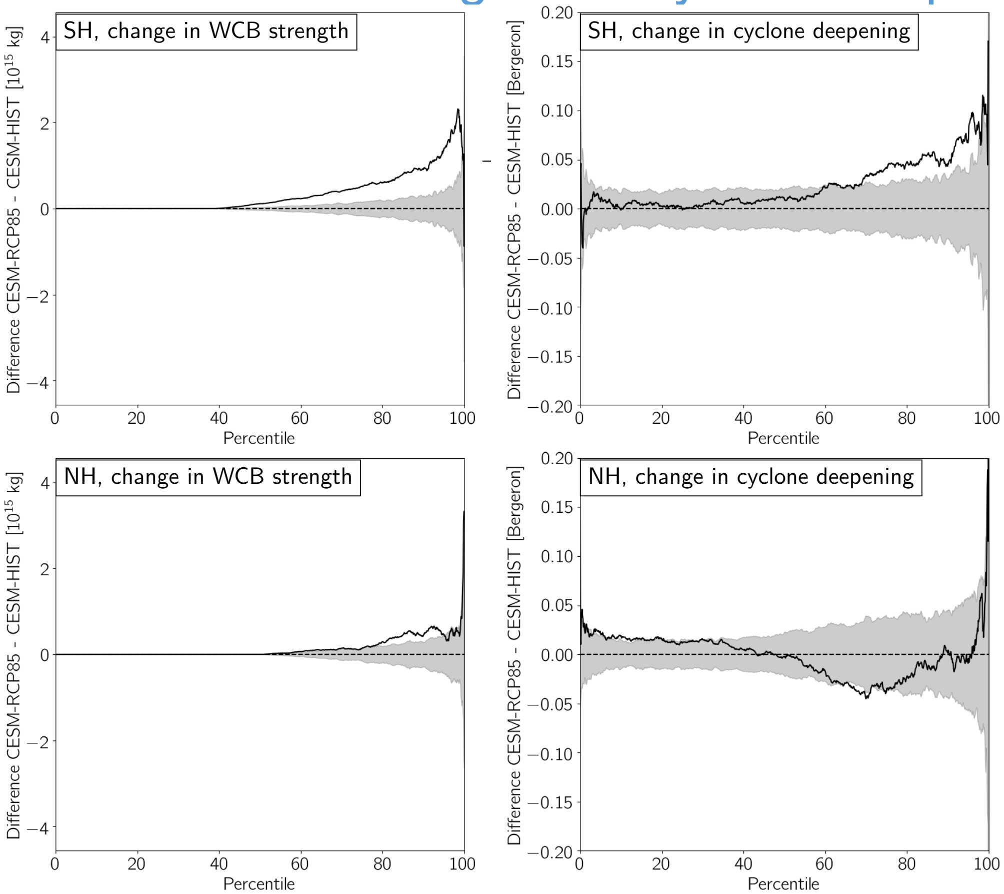

Percentile differences between CESM-RCP85 and CESM-HIST of the WCB strength associated with the cyclones (in 10^{15}kg) and the cyclone deepening rates (in Bergeron), together with the 95% confidence interval (grey shading) in the SH (top) and NH (bottom).

- In the Southern Hemisphere (SH), WCB strength and the cyclone deepening rate increase in the future climate for moderate and strong cyclones.
- In the Northern Hemisphere (NH), WCB strength also increases, but to a smaller extent, and there are no significant changes in the cyclone deepening rates.
- The different responses in terms of cyclone deepening to increased WCB intensities are consistent with the opposite changes in near-surface baroclinicity expected with global warming (increase in the SH, favourably interacting with the moist dynamics to create stronger storms, and decrease in the NH, counteracting the effects of the moist dynamics, e.g., Harvey et al. 2014).

How will the properties and structure of explosively intensifying cyclones with strong WCBs (C1 cyclones) change in a future climate?

WCB trajectory frequency at low levels, SLP & PV at 250hPa

Precipitation, TH at 850 hPa, wind at 250 hPa

WE cross section of PV & TH through cyc. centre

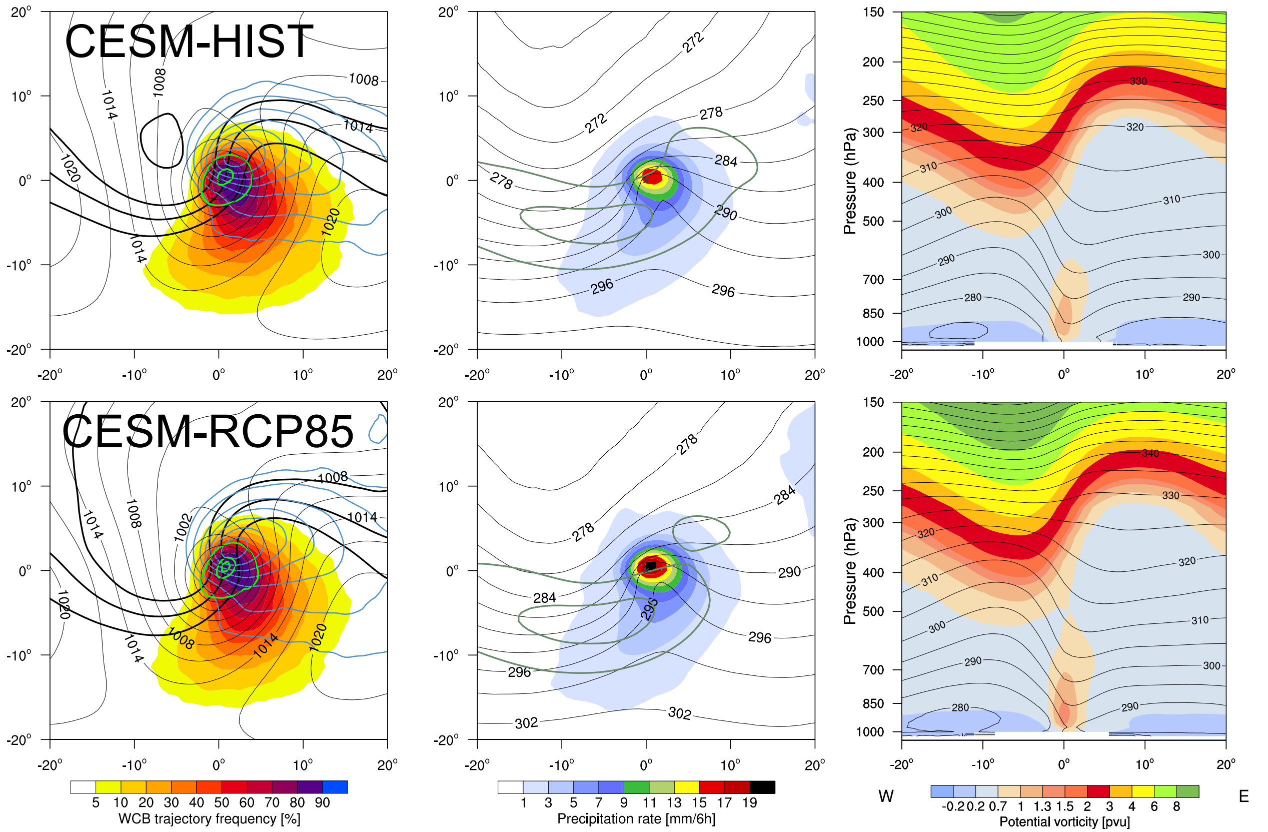

Composites of C1 cyclones in NH winter in the middle of the 24h period of strongest deepening in CESM-HIST (top) and CESM-RCP85 (bottom).

- C1 cyclones will be associated with even stronger WCBs, more WCB-related diabatic PV production, increased precipitation and to become warmer, moister and slightly more intense, with little changes in UL forcing for ascent.

Conclusions:

- Extratropical cyclones will be more diabatic in a warmer climate.
- WCB-related PV production will be even more important for explosive cyclone intensification.
- The interplay between dry and moist dynamics is important to understand how climate change affects cyclone intensification.

Foehn frequencies in Altdorf, Switzerland

(1) Can machine learning (ML) predict monthly foehn frequencies based on meso-scale features?

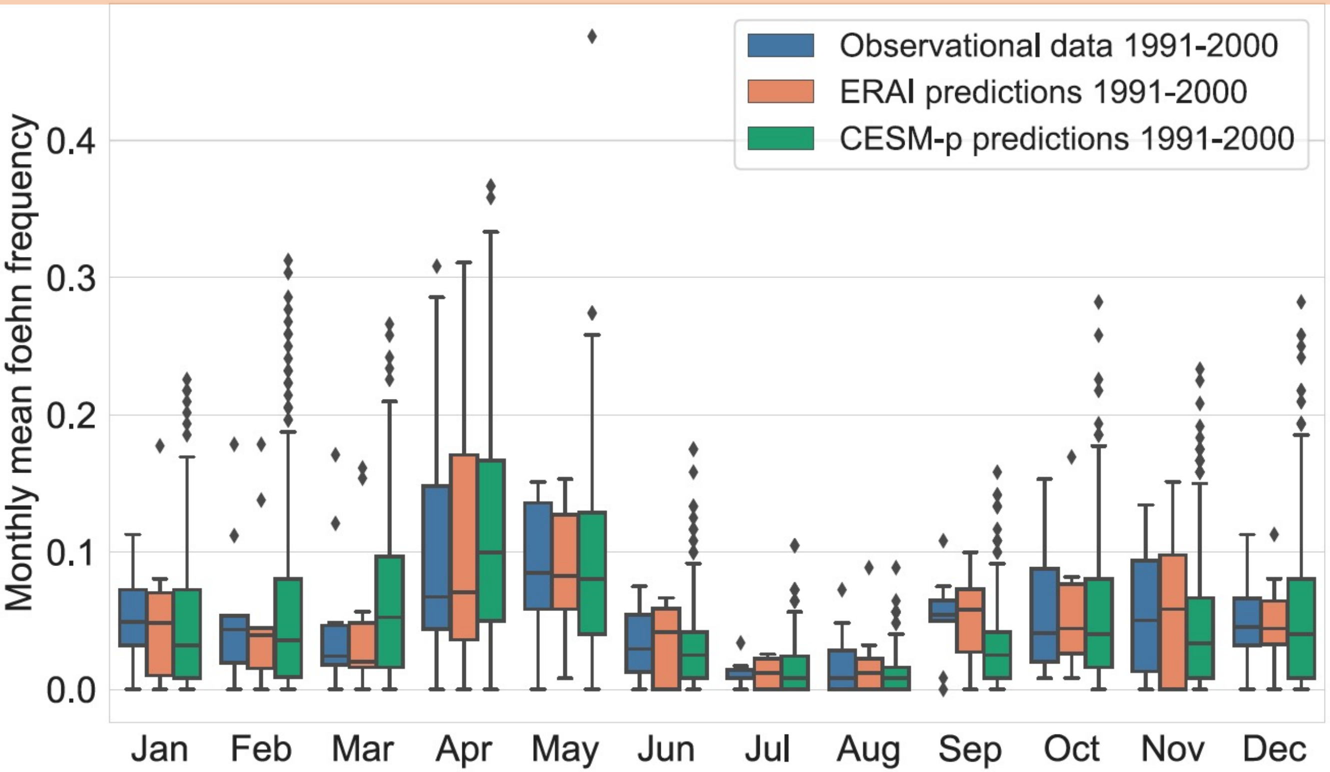

Observed monthly foehn frequencies in Altdorf between 1991-2000 as basis

Train a machine-learning (ML) algorithm (XGBoost) based on ERA-Interim features for the period 1979-1990, 2001-2019

Apply this ML algorithm to ERA-Interim period 1991-200 and to 700 years present-day CESM1 data

ML-based predictor can successfully be applied to ERA-Interim and CESM1

Foehn frequencies in Altdorf, Switzerland

(2) Do foehn frequencies change from present-day to future climate?

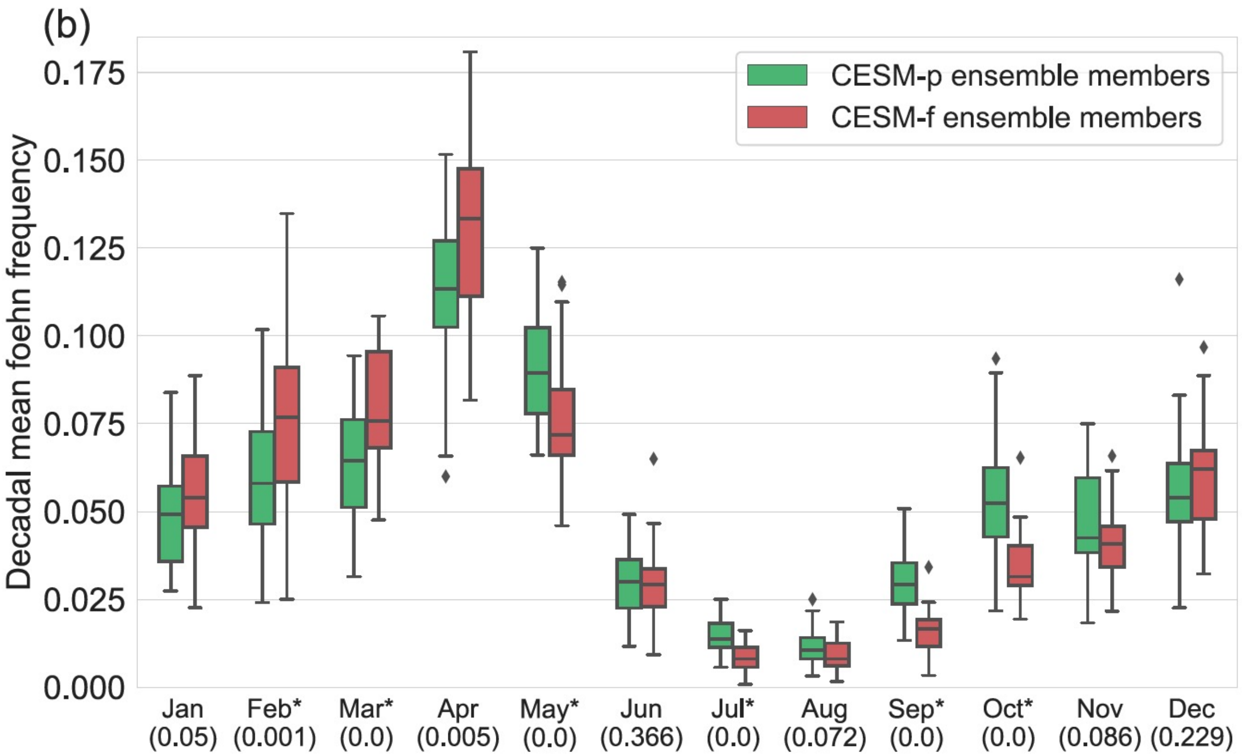

Compare predictions of monthly foehn frequencies between 700 years of

- *present-day CESM1 (1991-2000)*
- *future CESM (2091-2100)*

Significant shifts in foehn frequencies in spring (March-May)

Foehn frequencies in Altdorf, Switzerland

(3) Which ERA-Interim/CESM1 features are important for ML algorithm (feature importance)?

Variable	Description	Pressure levels (hPa)	Features (No.)
ΔSLP	Sea level pressure differences	Sea level	5356
ΔZ	Geopotential height differences	850, 700	10 712
$\Delta\theta_{hor}$	Horizontal potential temperature differences	850	5356
$\Delta\theta_{ver}$	Vertical potential temperature differences	850–900, 700–900	208
U	Zonal wind component	700, 500	208
V	Meridional wind component	700, 500	208

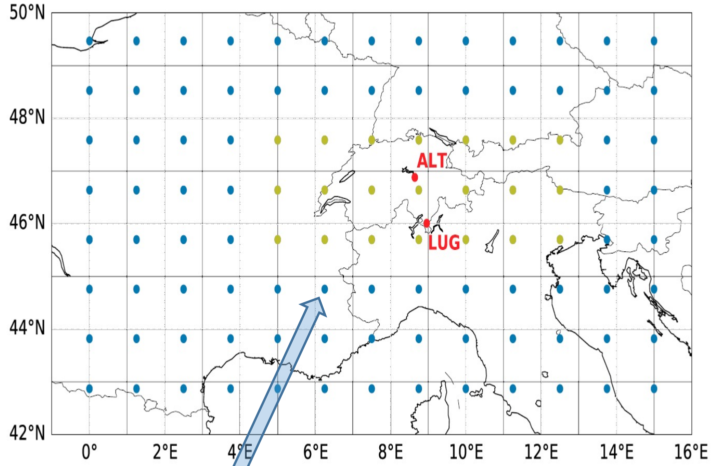

domain and grid points on which ERA-Interim and CESM1 features are extracted

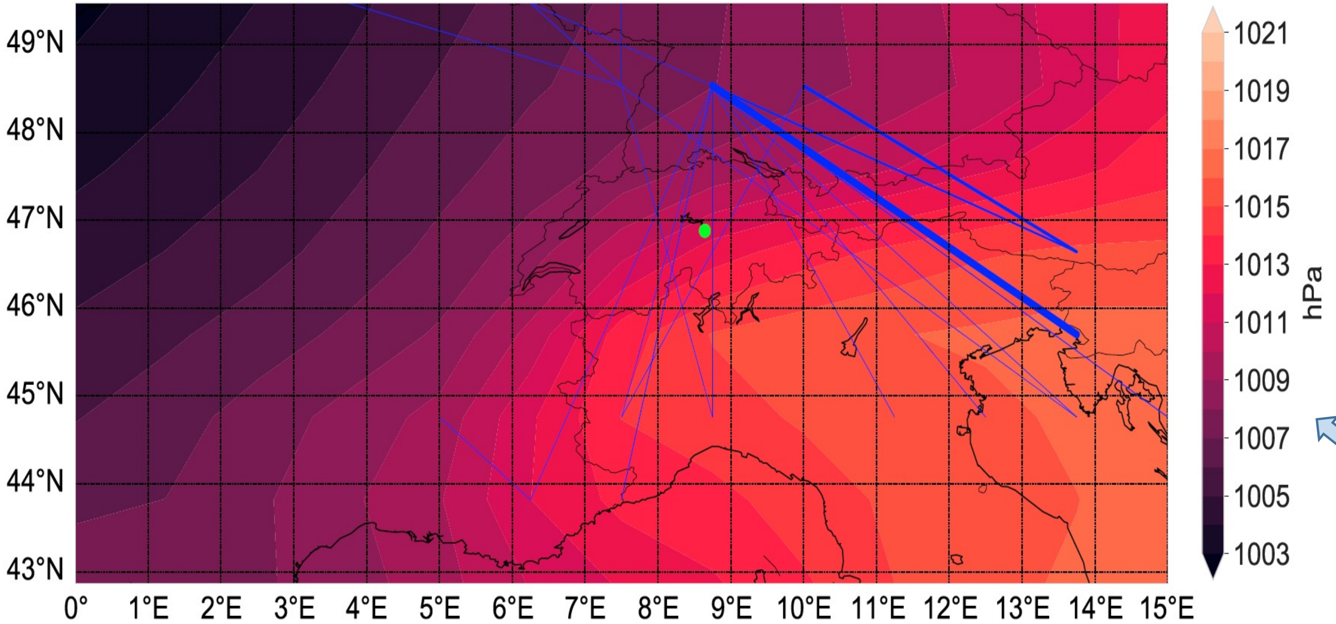

Importance of SLP differences, the thicker the line the more important